Orientation of Molecular Segments by Plastic Deformation of Glassy Polycarbonate

Marcel Utz,† Marco Tomaselli,† Richard R. Ernst,‡ and Ulrich W. Suter*,†

Institut für Polymere and Laboratorium für Physikalische Chemie, Eidgenössische Technische Hochschule, CH-8092 Zürich, Switzerland

Received November 22, 1995; Revised Manuscript Received December 29, 1995[⊗]

ABSTRACT: Annealed, selectively ^{13}C-labeled Bisphenol A polycarbonate samples were uniaxially compressed (compressive strain ca. 40%). One-dimensional static NMR spectra of the deformed samples were recorded at different orientations with respect to the magnetic field. The orientational distributions of the carbonate groups and the phenylene rings were determined through a fitting of the spectra by an expansion in Wigner rotation matrix elements. The data are explained quantitatively by an affine network-deformation model. The chains qualitatively behave as compressed random coils.

1. Introduction

The microscopic processes involved in the ductility of amorphous polymer materials and the mechanisms of plastic deformation at atomistic detail are still not fully understood, although a number of theoretical studies (e.g., see refs 1−6) and many experimental results have been reported in the literature. It is known from calorimetry that a large part of the deformation work is stored as internal energy in the polymer,[7,8] reflecting structural changes in the material, such as orientational and conformational ordering, induction of density fluctuations, or deformation-induced crystallization or melting.[9,10] Direct observation of these microscopic changes would contribute toward an understanding of the mechanism of plastic deformation. A first step in investigating plastic deformation consists of determining the orientational distribution induced in the material.

Many efforts have been reported to measure orientational distributions of molecular segments in oriented polymer samples by birefringence,[11,12] by Raman[13] and infrared spectroscopy,[14] by fluorescence depolarization,[15] by various NMR techniques,[16−21] and by neutron scattering.[22] In the case of drawn polymer fibers, it is generally found that the polymer chains align with the fiber axis, and the distribution retains cylindrical symmetry. Chmelka, Schmidt-Rohr, and Spiess[20] have determined the orientation of phenylene rings and carboxyl groups in biaxially drawn industrial films of semicrystalline poly(ethylene terephthalate) using the sample-reorientation technique introduced by Carter, Alderman, and Grant[23] and Henrichs.[24] They found that the planes of both the phenylene rings and the carboxyl groups tend to align strongly with the sheet plane.

Most structural studies have focused so far on samples deformed in tension, where the accessible strain range is limited by either brittle fracture or the advent of inhomogeneous deformation due to strain-softening effects. Many measurements have been performed at temperatures *above the glass transition*, and their results are of little use in understanding the process of plastic deformation in amorphous polymer glasses. In this contribution, we report the determination of the distribution of segmental orientations, induced by uniaxial compression at room temperature, in selectively ^{13}C-labeled Bisphenol A polycarbonate by solid-state NMR spectroscopy. The analysis is based on one-dimensional static ^{13}C chemical shift anisotropy (CSA) patterns. We employ compression, rather than dilatation, to induce large homogeneous plastic deformation. Mechanical instabilities such as fracture, necking and crazing, are thus avoided and very large sample deformations can be achieved.

2. Theory

The orientational distribution of an ensemble of rigid segments of the polymer chain can be described by the probability density function $P(\alpha\beta\gamma)$ where the differential probability of finding a segment at a particular orientation is given by

$$\mathrm{d}W(\alpha\beta\gamma) = P(\alpha\beta\gamma)\sin\beta\,\mathrm{d}\beta\,\mathrm{d}\alpha\,\mathrm{d}\gamma \qquad (1)$$

The Euler angles α, β, and γ relate the sample frame to the segmental frame, which is chosen to be coincident with the principal axes frame of the interaction tensor that is responsible for the observed spectrum $S(\omega)$. The definition of the Euler angles follows the conventions of Brink and Satchler.[27] The spectrum $S(\omega)$ can be observed at different orientations R_S of the sample with respect to the laboratory frame, for instance by rotating it by an angle φ about its y axis:

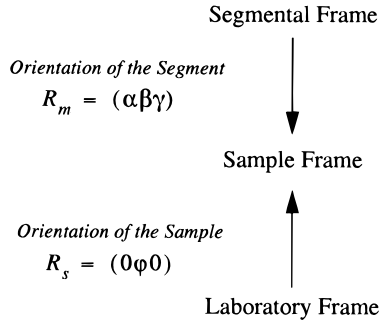

The function $P(\alpha\beta\gamma)$ can be derived, in principle, from measured spectral or scattering data, provided they are sufficiently sensitive to segmental orientation. We introduce the function ζ that projects the orientational distribution function onto a set of experimental observ-

† Institut für Polymere.
‡ Laboratorium für Physikalische Chemie.
[⊗] Abstract published in *Advance ACS Abstracts,* February 15, 1996.

0024-9297/96/2229-2909$12.00/0

ables $S(\omega)$ which, in our case, represents a spectrum or a series of spectra:

$$S(\omega) = \zeta[P(\alpha\beta\gamma)] \tag{2}$$

The relationship in eq 2 between the orientational distribution function and the spectrum is linear in the sense that

$$\zeta[aP + bQ] = a\zeta[P] + b\zeta[Q] \tag{3}$$

In general, it is not possible to invert eq (2) analytically. The decomposition of $P(\alpha\beta\gamma)$ into a suitable set of orientational basis functions provides a possible solution to this problem. The spectra corresponding to the individual orientational basis functions can be computed, and the linearity stated in eq 3 makes it possible to find a set of expansion coefficients by comparing the "basis spectra", thus obtained, to the measured data. The functions of choice are the Wigner matrix elements $D^l_{mn}(\alpha\beta\gamma)$, which are defined as the matrix elements of the general rotation operator $D(\alpha\beta\gamma)$[25−27]

$$D^l_{mn}(\alpha\beta\gamma) = \langle lm|D(\alpha\beta\gamma)|ln\rangle \tag{4}$$

They have been used for this purpose by McBrierty, who also demonstrated how the expansion coefficients can be found from experimental data.[28] Hentschel *et al.*[16,26] have described the elucidation of orientational distributions from NMR line shapes using Wigner matrix elements. Essentially the same method of analysis has been applied by Harbison, Vogt, and Spiess[17] to interpret rotor-synchronized MAS spectra of oriented polymer samples. Roe and Krigbaum[29] had previously suggested the use of Legendre polynomials and spherical harmonics, which are both (to within a constant factor) equal to certain Wigner matrix elements, for expanding axially symmetric distributions.

We take into account all Wigner matrix elements up to a certain order for the expansion, rather than to restrict it to the spherical harmonics, although this would have been sufficient for the interpretation of the experimental results reported here. $P(\alpha\beta\gamma)$ is expanded into the (infinite) series

$$P(\alpha\beta\gamma) = \sum_{l,\,m,\,n} C^l_{mn} D^l_{mn}(\alpha\beta\gamma) \tag{5}$$

where C^l_{mn} are the scalar expansion coefficients. The convergence of this series is rapid if the distribution is smooth. It is known that the ensemble averages of the Wigner matrix elements can be viewed as order parameters of the distribution,[20]

$$\langle D^l_{mn}\rangle = \frac{C^l_{mn}}{(2l+1)} \tag{6}$$

with values limited to the interval $[-1, 1]$.

Insertion of eq 5 into eq 2 leads to the corresponding expansion of the spectrum

$$\begin{aligned} S(\omega) &= \sum_{l,m,n} C^l_{mn}\zeta[D^l_{mn}(\alpha\beta\gamma)] \\ &= \sum_{l,m,n} C^l_{mn} S^l_{mn}(\omega) \end{aligned} \tag{7}$$

with the basis spectra $S^l_{mn}(\omega) \equiv \zeta[D^l_{mn}(\alpha\beta\gamma)]$. A reorientation of the *sample* corresponds to the application of a rotation R_S after the rotation defining the orientation of the segment has been carried out. Therefore, the transformed Wigner matrix elements are

$$D^{Rl}_{mn}(\alpha\beta\gamma) = \langle lm|D(R_S)D(\alpha\beta\gamma)|ln\rangle \tag{8}$$

Insertion of the closure relation into eq 8 yields

$$\begin{aligned} D^{Rl}_{mn}(\alpha\beta\gamma) &= \sum_{J,k} \langle lm|D(R_S)|Jk\rangle\langle Jk|D(\alpha\beta\gamma)|ln\rangle \\ &= \sum_k D^l_{mk}(R_S) D^l_{kn}(\alpha\beta\gamma) \end{aligned} \tag{9}$$

The spectra to be expected at a sample orientation specified by the rotation R_S can be found from eqs 9 and 7:

$$\begin{aligned} S^R(\omega) \equiv R_S S(\omega) &= \sum_{l,k,n} [\sum_m C^l_{mn} D^l_{mk}(R_S)] S^l_{kn}(\omega) \\ &= \sum_{l,k,n} C^{Rl}_{kn} S^l_{kn}(\omega) \end{aligned} \tag{10}$$

Unfortunately, the basis spectra are in general not orthogonal to each other, and therefore, the projections A^{Rl}_{mn}, with

$$A^{Rl}_{mn} = \int_\Omega S^R(\omega) S^l_{mn}(\omega)\, \mathrm{d}\omega \tag{11}$$

are not equal to the desired orientational expansion coefficients C^{Rl}_{kn} in eq 10. A relation between the two sets is found by inserting eqs 7 and 10 into eq 11:

$$\begin{aligned} A^{Rl}_{mn} &= \int_\Omega [\sum_{l',m',n'} C^{Rl'}_{m'n'} S^{l'}_{m'n'}(\omega)] S^l_{mn}(\omega)\, \mathrm{d}\omega \\ &= \sum_{l',m',n'} C^{Rl'}_{m'n'} \int_\Omega S^{l'}_{m'n'} S^l_{mn}\, \mathrm{d}\omega = \sum_{l',m',n'} C^{Rl'}_{m'n'} G^{l'\ \ l}_{m'n'mn} \end{aligned} \tag{12}$$

By arranging the sets of coefficients A^{Rl}_{mn} and C^{Rl}_{mn} into column vectors $\mathbf{a}^R$ and $\mathbf{c}^R$, it becomes possible to express the above relation in terms of a multiplication with the matrix $\mathbf{G}$:

$$\mathbf{a}^R = \mathbf{G}\mathbf{c}^R \tag{13}$$

In addition, a unitary matrix $\mathbf{D}^R$ describing the rotation of the coordinate frame can be constructed from the Wigner matrix elements such as to reproduce the transformation law eq 10, leading to

$$\mathbf{a}^R = \mathbf{G}\mathbf{D}^R\mathbf{c} \tag{14}$$

where the vector $\mathbf{c}$, which comprises the expansion coefficients C^l_{mn}, can be found by inverting the matrix $\mathbf{G}\mathbf{D}^R$. In general, however, some of the basis spectra will be linearly dependent, leading to a singular matrix $\mathbf{G}$, and there will not be a unique solution to the problem. Singular value decomposition[30] can be applied to find a particular solution and a set of kernel basis vectors in the coefficient vector space. If several spectra at different orientations R of the sample with respect to the external magnetic field have been recorded, the indeterminacy can be reduced by finding the set of expansion coefficient vectors consistent with all spectra, corresponding to the intersection of the individual solution spaces. Besides, *a priori* knowledge of the symmetry of the underlying orientational distribution can be used, reducing the number of feasible basis

functions. As the orientational distribution function is always real, complex conjugate Wigner matrix elements must contribute equally to the expansion. This gives rise to the condition

$$C^l_{mn} = (-1)^{m-n} C^l_{-m-n} \tag{15}$$

The subspace of symmetry-compatible coefficient vectors has to be intersected with the solution spaces obtained from the spectra to yield the final solution.

The sensitivity of the expansion coefficients to noise in the spectral data can be estimated from the matrix of second derivatives **H** (Hessian matrix) of

$$\chi^2 = \frac{1}{N_R \Omega} \sum_R \int_\Omega (\mathbf{s}^T(\omega)\mathbf{D}^R\mathbf{c} - S^R(\omega))^2 \, \mathrm{d}\omega \tag{16}$$

where $\mathbf{s}^T(\omega)$ is a row vector containing the basis spectra, and the sum extends over all N_R orientations of the sample that have been measured. Ω denotes the width of the spectral domain that contains the relevant features. The Hessian matrix is given by

$$\mathbf{H} = \left(\frac{\partial^2[\chi^2]}{\partial c_i \partial c_j}\right) = \frac{2}{N_R \Omega} \sum_R (\mathbf{D}^R)^T \mathbf{G} \mathbf{D}^R \tag{17}$$

If symmetry constraints apply, **H** can be projected onto the subspace of symmetry-compatible coefficient vectors

$$\mathbf{H}_S = \mathbf{Q}\mathbf{H}\mathbf{Q}^T \tag{18}$$

where **Q** is a unitary matrix whose rows form a basis of the symmetry-compatible subspace. Diagonalization of $\mathbf{H}_S$ leads to a set of normal coordinates **U** and corresponding eigenvalues

$$(\mathbf{U}\mathbf{H}_S\mathbf{U}^T)_{ij} = \lambda_i \delta_{ij} \tag{19}$$

The variation of χ^2 that results from a change $\Delta\mathbf{c}$ in the coefficients is, to second order,

$$\Delta\chi^2 \cong \frac{1}{2}\Delta\mathbf{c}^T\mathbf{H}\Delta\mathbf{c} = \frac{1}{2}\sum_i \lambda_i \Delta b_i^2 \tag{20}$$

where b_i are the expansion coefficients in the eigenbasis of $\mathbf{H}_S$ given by $\mathbf{b} = U\mathbf{Q}\mathbf{c}$. Let σ^2 be the variance in those regions of the spectra that contain only random noise. A comparison of $\Delta\chi^2$ and σ^2 then gives an estimate for the errors in the coefficients due to noise in the spectral data:

$$\Delta b_i \le \sqrt{2\sigma^2/\lambda_i} \tag{21}$$

The estimated errors in the coefficient space are found by the transformation $\Delta\mathbf{c} = \mathbf{Q}^T\mathbf{U}^T\Delta\mathbf{b}$. Some of the eigenvalues of $\mathbf{H}_S$ might be zero, or very small. The corresponding coefficients cannot be determined from the data at hand and should be set to zero.

In the present work, the static one-dimensional NMR spectra of uniaxially deformed polycarbonate samples, selectively enriched with ^{13}C at chemically equivalent sites, have been recorded under strong proton decoupling. Due to the large distances between the ^{13}C labels in the samples, the carbon−carbon dipolar couplings can be neglected, and the anisotropic chemical shift alone is responsible for the observed line shape.

The observable part of the CSA tensor in the segmental frame of reference has orthorhombic symmetry (point group D_{2h}). The same point group applies to the orientational distribution function in the sample frame of reference due to the homogeneity of the deformation. Thus, the orientational distribution function must be invariant upon a 180° rotation R_π of the CSA tensor about its principal axes as well as upon a corresponding rotation of the sample. In the latter case, the transformation law for the Wigner matrix elements is given in eq 9, while for a rotation of the CSA tensor it is

$$D^{Rl}_{mn}(\alpha\beta\gamma) = \sum_k D^l_{mk}(\alpha\beta\gamma) D^l_{kn}(R_\pi) \tag{22}$$

The condition that the orientational distribution function be invariant under the transformations (9) and (22) leads to the symmetry constraints

$$C^l_{mn} = (-1)^{l+m} C^l_{-mn}, \qquad C^l_{mn} = (-1)^m C^l_{mn}$$
$$C^l_{mn} = (-1)^{l+n} C^l_{m-n}, \qquad C^l_{mn} = (-1)^n C^l_{mn} \tag{23}$$

The mirror planes in the point groups give rise to the additional constraints

$$C^l_{mn} = C^l_{-mn} = C^l_{m-n} \tag{24}$$

It follows from eqs 23 and 24 that only even values of m, n, and l need to be considered and that the coefficients are independent of the signs of m and n.

3. Experimental Section

Measurements were carried out with two samples of Bisphenol A polycarbonate selectively enriched with ^{13}C (>99%): sample 1 at the carbonate carbon ("carbonate label") and sample 2 at the (nonprotonated) phenylene carbon directly bonded to the carbonate unit ("phenylene label"), as shown in Figure 1a. The carbonate-labeled material was enriched at each carbonate unit, the phenylene-labeled material twice at every second Bisphenol A unit. The synthesis and the detailed characterization of both polymers are given elsewhere;[31] here it suffices to note that sample 1 is of molecular weight M_w = 30 500 whereas sample 2 is 31 700; both are characterized by M_w/M_n of 1.5.

The polycarbonate samples were dissolved in methylene chloride (5% w/v) and then precipitated by casting the solutions into the 10-fold volume of heptane. The polymer was separated by filtration and washed several times with pure heptane. The material thus obtained was dried in vacuum (80 mbar) at 60 °C for at least 24 h. Dense, clear cylindrical samples of approximately 7 mm length were obtained by compression into a cylindrical die of 5 mm diameter under a load of 7.5 MPa at 200 °C and under vacuum (<0.5 mbar) for 25 min. The samples were subsequently compressed at room temperature in another, similar die of larger diameter (7 mm) to induce a plastic uniaxial compression to 60 ± 5% of their original length, corresponding to a compressive strain of $\epsilon = -0.40 \pm 0.05$.

Static NMR measurements were performed on a home-built spectrometer operating at a proton resonance frequency of 220 MHz. The radio-frequency field strengths on both channels were matched to 50 kHz for all experiments. Carbon-13 chemical shift anisotropy patterns were recorded after 1 ms ^{1}H−^{13}C Hartmann−Hahn cross-polarization. Measurements were carried out at 135 ± 5 K with a home-built probe assembly using cooled nitrogen as a cryogen. The samples were oriented with the axis of compression inclined at angles of 0, 45, and 90° with respect to the external magnetic field.

Basis spectra up to sixth order ($l \le 6$; $|m|, |n| \le 6$) were included in the analysis. Gaussian broadening functions with a full width at half-height (fwhh) of 300 Hz were applied to

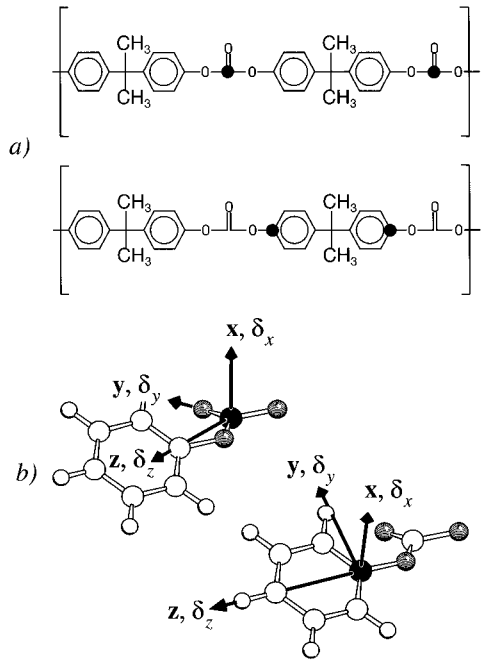

Figure 1. (a) Repeating units of Bisphenol A polycarbonate. The heavily marked atoms indicate the positions of the ^{13}C labels in the two different samples. (b) Definition of the molecular reference frames. The orientation of the principal axes has been chosen in accordance with Henrichs *et al.*[36] This choice has recently been supported by CSA-dipole tensor correlation experiments in doubly ^{13}C enriched polycarbonate samples.[31] The principal axis of the CSA tensor that is parallel to the local chain direction has been chosen as the *z* axis. δ_x, δ_y, and δ_z denote the corresponding principal values of the chemical shift tensor, which are given in Table 1.

Table 1. Principal Values of the Chemical Shift Tensor (ppm Relative to TMS) Used for the Analysis, Previously Determined from Low-Temperature 1D Powder Spectra of Undeformed Samples[31]

principal value of the chemical shift tensor	carbonate label	phenylene label
δ_z	234	233
δ_y	124	128
δ_x	84	75

the computed spectra to represent unidentified line broadening contributions. The principal values of the chemical shift tensor have been determined previously on undeformed samples[31] and are given in Table 1.

4. Results and Discussion

Measured spectra are shown in Figure 2 along with fitted theoretical spectra up to sixth order. The small peaks to the right of the CSA tensor line shapes are due to natural abundance aliphatic ^{13}C and are irrelevant for the analysis undertaken here. The experimental data are reproduced within experimental error by the fits, except for a slight deviation for the carbonate-labeled sample at 45° (Figure 2a). However, as will be made clear in the following, a reasonable fit is not a sufficient criterion to judge the accuracy of the derived orientational distribution function.

A molecular coordinate frame has been chosen for each of the two labeled sites, coinciding with the eigenframes of the chemical shift tensors, as shown in Figure 1b. The non-zero order parameters for $l \leq 6$ are given in Table 2. The errors indicated have been estimated from the random-noise level in the spectra using the eigenvalues of the Hessian matrix and eq 21.

No satisfactory reproduction of the measured spectra could be achieved with a uniaxial orientational distribution, represented by the terms D^l_{0m}. Some dependence of the orientational distribution on the Euler angle α seems to exist, which is in contradiction with the attempted uniaxial deformation. It is unclear whether this is due to imperfections in the experimental procedure or whether it is a basis-set truncation effect.

There are $(2l + 1)^2$ different Wigner matrix elements D^l_{mn}. The symmetry constraints eqs 23 and 24 rule out

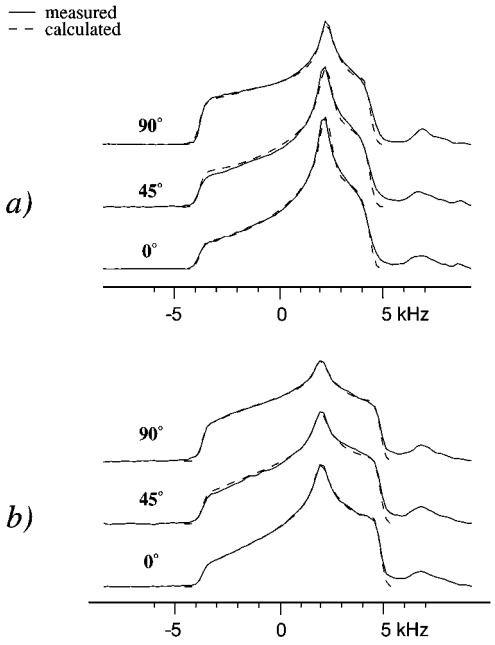

Figure 2. Solid lines: 1D powder spectra measured on uniaxially compressed ($\epsilon = -0.40 \pm 0.05$) samples, ^{13}C-labeled at the carbonate site (a) and at the phenylene site (b). Broken lines: corresponding spectra back-calculated from the orientational distributions with Wigner-matrix elements to sixth order. The angle between the compression direction and the magnetic field vector is indicated in the spectra.

Table 2. Order Parameters $\langle D^l_{mn} \rangle$ Determined by Taking into Account Wigner-Matrix Elements up to Sixth Order

l	*m*	*n*	carbonate label	phenylene label
0	0	0	1	1
2	0	0	−0.056 ± 0.003	−0.059 ± 0.001
2	2	0	0.004 ± 0.010	−0.003 ± 0.010
2	0	2	−0.026 ± 0.008	0.021 ± 0.008
2	2	2	−0.009 ± 0.007	0.028 ± 0.003
4	0	0	−0.014 ± 0.018	−0.021 ± 0.007
4	2	0	−0.015 ± 0.019	−0.020 ± 0.002
4	4	0	−0.014 ± 0.004	−0.029 ± 0.001
4	0	2	0.000 ± 0.006	−0.004 ± 0.005
4	2	2	0.004 ± 0.012	−0.005 ± 0.001
4	4	2	−0.002 ± 0.005	−0.010 ± 0.001
4	0	4	0.004 ± 0.020	−0.004 ± 0.011
4	2	4	0.006 ± 0.011	−0.003 ± 0.006
4	4	4	0.004 ± 0.006	−0.005 ± 0.005
6	0	0	0.008 ± 0.017	0.000 ± 0.001
6	2	0	0.001 ± 0.002	−0.003 ± 0.002
6	4	0	0.007 ± 0.001	−0.002 ± 0.002
6	6	0	0.002 ± 0.012	−0.004 ± 0.007
6	0	2	0.001 ± 0.008	0.003 ± 0.007
6	2	2	0.002 ± 0.001	0.004 ± 0.003
6	4	2	0.001 ± 0.010	0.003 ± 0.001
6	6	2	0.003 ± 0.004	0.006 ± 0.001
6	0	4	0.000 ± 0.005	−0.001 ± 0.003
6	2	4	0.000 ± 0.001	0.001 ± 0.011
6	4	4	0.000 ± 0.009	0.001 ± 0.001
6	6	4	0.000 ± 0.010	0.002 ± 0.004
6	0	6	−0.020 ± 0.001	0.008 ± 0.001
6	2	6	−0.005 ± 0.004	0.004 ± 0.001
6	4	6	−0.017 ± 0.012	0.003 ± 0.005
6	6	6	−0.008 ± 0.001	0.007 ± 0.004

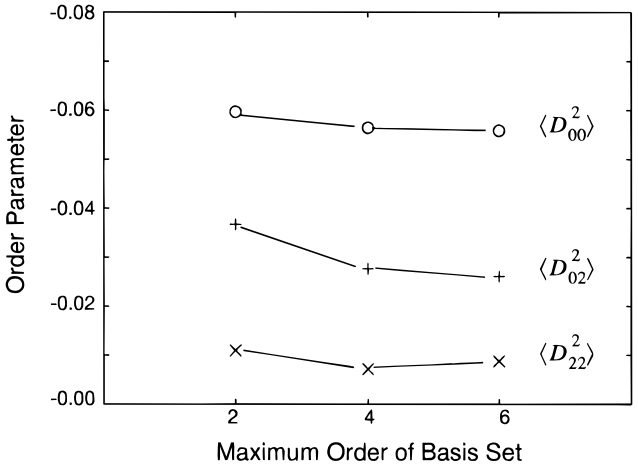

Figure 3. Order parameters with $l = 2$ obtained with basis sets truncated at terms of the order indicated on the horizontal axis.

odd l. For even values of l, they reduce the number of independent coefficients to $(l/2 + 1)^2$. Thus, taking into account Wigner matrix elements up to $l = 6$ corresponds to $1 + 4 + 9 + 16 = 30$ independent parameters.

For both labels, 12 of the 30 eigenvalues of the Hessian matrix $\mathbf{H}_S$ of order 6 were found to be practically zero. The corresponding coefficients were arbitrarily set to zero, leaving 18 relevant parameters in the fit. This choice leads to the least anisotropic orientational distribution function that is consistent with the spectral data.

The order parameters were found to vary slightly when the analysis was carried out with the smaller basis sets $l \leq 4$ and $l \leq 2$. This is due to the linear dependence and the nonorthogonality of the basis spectra. Cross terms in the Hessian matrix make it possible to compensate truncation errors by adjusting the coefficients of lower order. The accuracy of the orientational distribution, therefore, cannot be evaluated from the quality of the fit alone; the coefficients must also be stable with regard to an extension of the basis. It is evident from Figure 3 that this condition is already well met by the order parameters with $l = 2$.

The distributions of angles between the compression direction and the principal axes of the chemical shift tensor, calculated from the orientational distributions, are visualized in Figures 4 and 5. The vectors along the main chain (Figures 4a and 5a) tend to orient perpendicular to the axis of compression, as expected from an affine deformation of the random coil under homogeneous compressive strain. The C═O bond vector and the phenylene ring-plane normal tend toward an orientation parallel with the macroscopic axis of compression (Figures 4c and 5c). The remaining directions (Figures 4b and 5b) show no clear tendency.

If the segments of a "freely jointed chain"[32] were subjected to the same affine transformation as the outside shape of the samples, an order parameter $\langle D^2_{00}\rangle \cong -0.2$ would result. The order parameters for the two molecular segments studied in this work have been found to be almost a factor of 4 below this value (cf. Table 2). The measured values for $\langle D^2_{00}\rangle$ correspond to a compression of a freely jointed chain by merely 8%, as opposed to the macroscopic plastic sample deformation of 45%. Thus the orientational ordering at the atomistic level does not quantitatively reflect the change in the outside shape of the sample. Either relaxation processes that tend to restore the isotropic

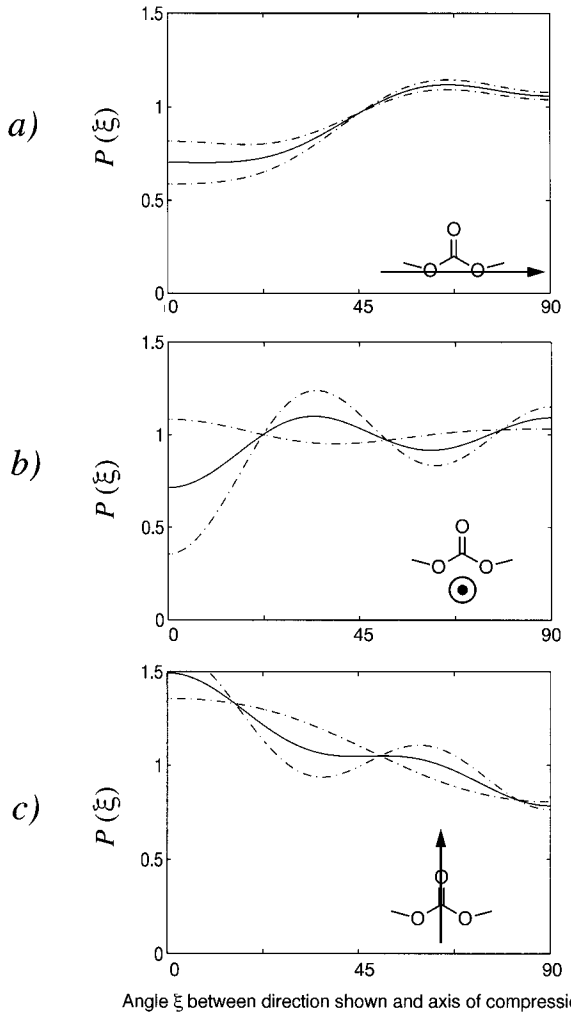

Figure 4. Distribution of angles (solid lines) between the axes of the carbonate molecular coordinate frame and the compression direction. The broken lines indicate the experimental uncertainty due to noise in the spectra.

distribution are still active at ambient temperature (150 K below T_g), or the mechanism of plastic deformation involves transitions that change the orientation of molecular segments to a lesser degree than would be expected from a simple affine transformation. Atomistic simulation studies on the deformation of polymer glasses[6] indeed predict the deformation to occur by plastic unit events comprising collective motions of many monomer units. This could explain the reduced order induced by the deformation.

Although no theoretical treatment of the development of orientational order in glassy polymers has appeared in the literature to date, the subject has received considerable attention in cross-linked networks above the glass transition. For a uniaxial deformation and a vector attached to a network chain "in the chain direction", Kuhn and Grün[32,33] found that the second Legendre polynomial of the cosine of the angle between this vector and the direction of deformation obeys the relationship

$$\langle D^2_{00}\rangle = \frac{1}{5N_x}\left(\lambda^2 - \frac{1}{\lambda}\right) \approx \frac{3\epsilon}{5N_x} \qquad \text{(for small } |\epsilon|) \qquad (25)$$

where $\lambda = 1 + \epsilon$ is the extension ratio and N_x, is the mean chain length between cross-links, measured in

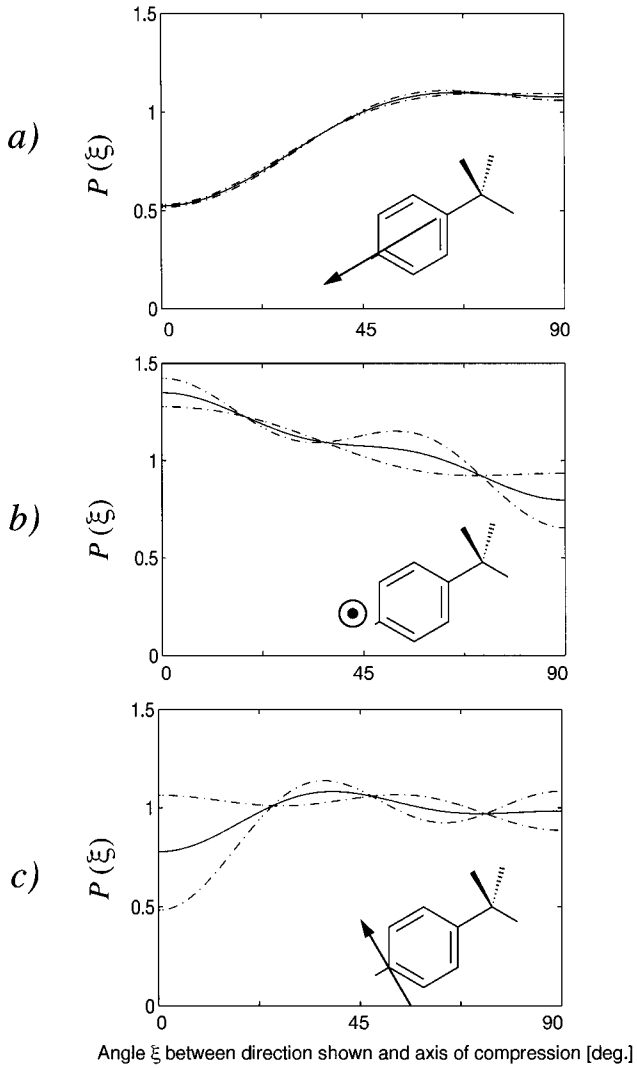

Figure 5. Distribution of angles (solid lines) between the axes of the phenylene molecular coordinate frame and the compression direction. The broken lines indicate experimental uncertainty.

number of Kuhn segments (i.e., equivalent freely-jointed segments). For convenience in comparison with the rest of this paper, we have replaced the second Legendre polynomial with the appropriate order parameter, formally equivalent for our choice of coordinates. More elaborate treatments have been published;[34] for the purpose of this communication, however, the original model is perfectly adequate.

The deformation of a glassy polymer is certainly different from that of a cross-linked network, typically in structural equilibrium under deformation. Nevertheless, one might consider, in analogy to the concept of an entanglement network in linear polymer melts, that a network of dynamical spatial constraints is active during the plastic flow of the material and produces the orientation finally observed in the plastically deformed glass. Equation 25 might thus be employed to estimate N_e (identified with N_x in the cross-linked network) from our experimental values for $\langle D_{00}^2 \rangle$. Taking the value obtained by NMR for $\langle D_{00}^2 \rangle$ of the carbonate group, where the direction of the vector "along" the chain can be readily identified with the chain direction, and a strain of $\epsilon = -0.40 \pm 0.05$, one obtains a value for N_e of 4.7 ± 0.7. For the determination of the molecular weight of a Kuhn segment we employ the experimental values listed by Fetters *et al.*[35] and obtain

$$\frac{M}{N} = \frac{\langle R^2 \rangle_0}{M} \frac{{m_0}^2}{{l_0}^2} = 370 \pm 80 \qquad (26)$$

which yields, together with our estimate of N_e, an "entanglement molecular weight" effective in glassy deformation of 1740 ± 650. This value is in surprisingly close agreement with the entanglement molecular weight relevant at the rubbery plateau in a melt, where it is ca. 1330.[35]

5. Conclusions

The described experiments on Bisphenol A polycarbonate have shown that compressive deformation of polymers does not merely lead to an affine deformation of the polymer chains. The individual chains appear to have significant freedom to relax toward an unstrained conformation with less order than expected.

Solid-state carbon-13 NMR proved to be a valuable means of monitoring the segmental ordering. Already the analysis of one-dimensional line-shape functions provides sufficient information to allow the determination of a number of order parameters. Preliminary results have shown that more sophisticated two-dimensional experiments confirm the findings derived from the present study. A detailed analysis of two-dimensional ^{13}C spectra of compressionally deformed samples will be presented at a later occasion.

Acknowledgment. We gratefully acknowledge financial support by the Swiss National Science Foundation. We also thank Serge Santos for valuable discussions.

References and Notes

(1) Robertson, R. E. *J. Chem. Phys.* **1966**, *44*, 3950−3956.
(2) Yannas, I. V. *Proc. Int. Symp. Macromol.* **1975**, 265.
(3) Hutnik, M.; Argon, A. S.; Suter, U. W. *Macromolecules* **1993**, *26*, 1097−1108.
(4) Mott, P. H.; Argon, A. S.; Suter, U. W. *Phil. Mag. A* **1993**, *67*, 931−978.
(5) Mott, P. H.; Argon, A. S.; Suter, U. W. *Phil. Mag. A* **1993**, *68*, 537−564.
(6) Argon, A. S.; Bulatov, V. V.; Mott, P. H.; Suter, U. W. *J. Rheol.* **1995**, *39*, 377−399.
(7) Oleynik, E. F.; Salamatina, O. B.; Rudnev, S. N.; Shenogin, S. V. *Polym. Sci. U.S.S.R.* **1993**, *35*, 1532−1558.
(8) Hasan, O. A.; Boyce, M. C. *Polymer* **1993**, *34*, 5085−5092.
(9) Flory, P. J. *J. Chem. Phys.* **1947**, *15*, 396−408.
(10) Fox, T. G.; Flory, P. J.; Marshall, R. E. *J. Chem. Phys.* **1949**, *17*, 704−706.
(11) Yannas, I. V.; Lunn, A. C. *J. Polym. Sci. Part B: Polym. Phys.* **1971**, *9*, 611−615.
(12) Lunn, A. C.; Yannas, I. V. *J. Polym. Sci., Phys. Ed.* **1972**, *10*, 2189−2208.
(13) Citra, M. J.; Chase, D. B.; Ikeda, R. M.; Gardner, K. H. *Macromolecules* **1995**, *28*, 4007−4012.
(14) Read, B. E.; Stein, R. S. *Macromolecules* **1968**, *1*, 116−126.
(15) Monnerie, L. *Faraday Symp. Chem. Soc.* **1983**, *18*, 57−81.
(16) Hentschel, R.; Sillescu, H.; Spiess, H. W. *Polymer* **1981**, *22*, 1516−1521.
(17) Harbison, G. S.; Vogt, V.-D.; Spiess, H. W. *J. Chem. Phys.* **1987**, *86*, 1206−1218.
(18) Schmidt-Rohr, K.; Hehn, M.; Schaefer, D.; Spiess, H. W. *J. Chem. Phys.* **1992**, *97*, 2247−2262.
(19) Simpson, J. H.; Rice, D. M.; Karasz, F. E. *Macromolecules* **1992**, *25*, 2099−2106.
(20) Chmelka, B. F.; Schmidt-Rohr, K.; Spiess, H. W. *Macromolecules* **1993**, *26*, 2282−2296.

(21) Tzou, D. L.; Spiess, H. W.; Curran, S. *J. Polym. Sci., Part B: Polym. Phys.* **1994**, *32*, 1521−1529.
(22) Ramzi, A.; Zielinski, F.; Bastide, J.; Boué, F. *Macromolecules* **1995**, *28*, 3570−3587.
(23) Carter, C. M.; Alderman, D. W.; Grant, D. M. *J. Magn. Reson.* **1985**, *65*, 183−186.
(24) Henrichs, P. M. *Macromolecules* **1987**, *20*, 2099−2112.
(25) Wigner, E. *Group Theory and its Application To The Quantum Mechanics Of Atomic Spectra*; Academic Press: New York, 1959.
(26) Hentschel, R.; Schlitter, J.; Sillescu, H.; Spiess, H. W. *J. Chem. Phys.* **1978**, *68*, 56−66.
(27) Brink, D. M.; Satchler, G. R. *Angular Momentum*, 3rd ed.; Clarendon Press: Oxford, U.K., 1993.
(28) McBrierty, V. J. *J. Chem. Phys.* **1974**, *61*, 872−882.
(29) Roe, R. J.; Krigbaum, W. R. *J. Chem. Phys.* **1964**, *40*, 2608−2615.
(30) Press, W. H.; Teukolsky, S. A.; Vetterling, W. T.; Flannery, B. P. *Numerical Recipes in C*, 2nd ed.; Cambridge University Press: Cambridge, U.K., 1992.
(31) Tomaselli, M.; Robyr, P.; Meier, B. H.; Grob-Pisano, C.; Ernst, R. R.; Suter, U. W. In preparation.
(32) Flory, P. J. *Statistical Mechanics of Chain Molecules*, reprinted ed.; Hanser Verlag: Munich, 1989.
(33) Kuhn, W.; Grün, F. *Kolloid-Z.* **1942**, *101*, 248−271.
(34) Haliloglu, T.; Erman, B.; Bahar, I. *Polymer* **1995**, *36*, 4131−4134 and references cited therein.
(35) Fetters, L. J.; Lohse, D. J.; Richter, D.; Witten, T. A.; Zirkel, A. *Macromolecules* **1994**, *27*, 4639−4647.
(36) Henrichs, P. M.; Linder, M.; Hewitt, J. M.; Massa, D.; Isaacson, H. V. *Macromolecules* **1984**, *17*, 2412−2416.

MA951737P